Chapter 7

SYNAPTIC TRANSMISSION II

INTRODUCTION

Initial insights into synaptic function were obtained under experimental conditions that simplified the process of transmitter release and permitted quantitative analysis. We learned in the last chapter that these experiments led to the general conclusion that the release of synaptic vesicles is the key step in transmittal release, at least in most cases. This chapter will consider the process of transmitter release in some detail. It will be convenient to divide the process into several steps and consider them in sequence: (1) flux of calcium through the presynaptic membrane, (2) release and recycling of synaptic vesicles, and (3) diffusion of neurotransmitter in the synaptic cleft.

FLUX OF CALCIUM THROUGH THE PRESYNAPTIC MEMBRANE

Influx of calcium into the terminal. An important conclusion from early studies on synaptic transmission carried out with the frog neuromuscular junction was that transmission depends upon extracellular calcium concentration. Bathing the preparation in a calcium-free Ringer's solution blocked evoked EPPs leaving only small amplitude EPPs that could be attributed to spontaneous release. The relation between extracellular calcium concentration and EPP amplitude was subsequently examined in more detail by Dodge and Rahamimoff (1967) who plotted EPP amplitude as a function of

extracellular calcium concentration. Their plots indicated that transmitter release depends upon calcium concentration raised to the fourth power.

This dependence of transmitter release on intraterminal calcium concentration was subsequently confirmed using a synapse in the stellate ganglion of squid (Fig. 7-1). The advantage of this preparation is that both the pre- and postsynaptic elements of the synapse are very large, so they can both be impaled with microelectrodes. Miledi (1973) showed that injection of calcium directly into the presynaptic element results in transmitter release and a PSP recorded in the postsynaptic element. Llinás and Nicholson (1975) used a calcium-sensitive photoprotein called *aequorin* to study the dynamics of calcium flux in the presynaptic element. Aequorin was injected into the presynaptic element and flashes of light were used to monitor the time course of calcium flux into the terminal. These studies firmly implicated calcium flux from the extracellular fluid into the presynaptic element as an important step in transmitter release.

The mechanisms by which calcium enters the presynaptic terminal was quickly shown to depend upon voltage-gated channels in the presynaptic element. The depolarization caused by invasion of the action potential into the presynaptic terminal activates the voltage-gated channels and allows calcium to enter the terminal. Properties of the presynaptic calcium channels have been studied in the squid stellate ganglion preparation using voltage-clamp methods (Llinás et al., 1976, 1981a,b; Augustine et al., 1985a,b). Depolarization of the presynaptic axon caused a calcium current,

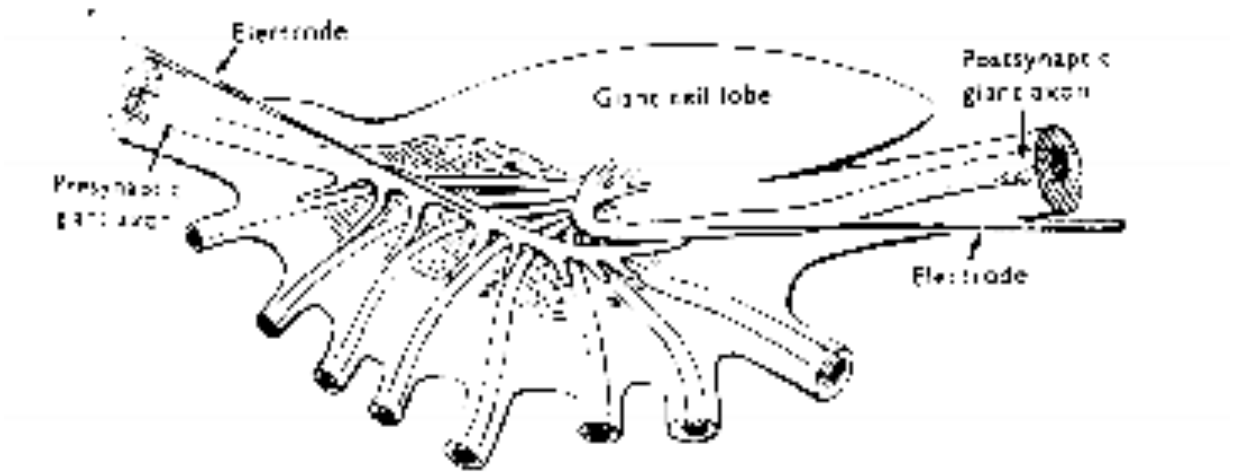

Figure 7-1. Squid stellate ganglion. The synapse between two giant axons in squid stellate ganglion allows individual electrodes to be placed in both the pre- and postsynaptic elements of the synapse. From (Bullock and Hagiawara, 1975).

I_{Ca}, to flow into the terminal. By recording from both the presynaptic and postsynaptic elements, it was possible to relate the features of I_{Ca} to the PSP. One important finding was a time delay of about 200 μsec between the onset of I_{Ca} and the postsynaptic response. Second, the amplitude of the PSP was a non-linear function of I_{Ca}. Third, the amplitude of I_{Ca} was, in turn, a non-linear function of the extracellular calcium concentration. Overall, data from squid stellate ganglion were consistent with the data from from neuromuscular junction in suggesting that transmitter release depends upon the fourth power of extracellular calcium. It is now known that there are serveral varieties of calcium channels involved in calcium influx to presynaptic terminals.

The advantage of both the frog neuromuscular junction and squid stellate ganglion preparations is that they are relatively accessible to experimental

manipulation. Extending work on intraterminal calcium dynamics to synapses in the central nervous system of vertebrates has depended upon the development of calcium-sensitive indicators. These are dyes that bind to calcium and fluoresce when the calcium is released. The extent of the fluorescence depends upon the wavelength of light used and the calcium concentration can be estimated by comparing the ratio of the fluorescence obtained using two different wavelengths of light. The calcium indicator used most commonly is called *Fura-2*, but a variety of compounds, including *mag-Fura-5* and *magnesium green*, differ in the kinetics of their binding to calcium and their sensitivities. Some results have been obtained using synapses with particularly large presynaptic elements. These include a synapse in the auditory system of rats (Borst and Sakmann, 1996). Slices through the hindbrain of rats contain the medial nucleus of the trapezoid body (MNTB). The MNTB is involved in processing information from the two ears (Fig. 7-2A). Neurons in this nucleus receive inputs that make large calyceal endings that can be impaled with an electrode. A second electrode is placed into the soma of an MNTB neuron so that presynaptic calcium currents can be compared to EPSCs in MNTB neurons (Fig. 7-2B). The findings were very much like those obtained in squid stellate ganglion. The calcium current was activated shortly after the presynaptic action potential reached its peak. EPSC amplitudes depended upon the extracellular calcium concentration raised to the fourth power (Fig. 7-2C). Estimates of the total calcium influx could be made and suggested that 13,000 calcium ions flow in for each vesicle released. This value is similar to estimates obtained for the squid stellate ganglion. At least 60 calcium channels open for each vesicle released, indicating that a fairly extensive *calcium domain* is created inside of the terminal.

Bernardo et al. (1996) used calcium indicators to study transmission in the synapse between granule cells and stellate cells in slices of rat cerebellar cortex. Granule cells have small somata and a few, short dendrites. They have

an axon that courses towards the surface of the cerebellum and then divides into two branches of equal length that course parallel to the cerebellar surface. They are called, accordingly, parallel fibers. Parallel fibers bear many varicosities which are presynapatic elements in *en passant* synapses that contact a variety of cell types in the outer layer of the cortex, including stellate cells. Stellate cells are electrotonically compact, so recordings from their somata provide reasonably accurate information of synaptic events occuring on their dendrites. The experiment Bernardo et al. did involved recording EPSCs from stellate cells while monitoring the activity in parallel fibers with both a calcium indicator, such as magnesium green, and a voltage sensitive dye. The dye is a small molecule that is soluble in membranes. It fluoresces at specific wavelengths, with the intensity of the fluorescence depending upon the membrane voltage. This experimental paradigm allowed simultaneous monitoring of the presynaptic membrane potential, the calcium concentration in the parallel fibers and EPSCs in stellate cells. The results obtained at room temperature were similar to those obtained in squid stellate ganglion and the rat MNTB. The calcium current occurred during the downstroke of the presynaptic action potential and preceded EPSCs by about 1.1 ms. However, repeating the experiment at physiological temperatures produced quantitatively different results in that the calcium current occurred near the peak of the action potential and led the EPSC by just 60 μsec.

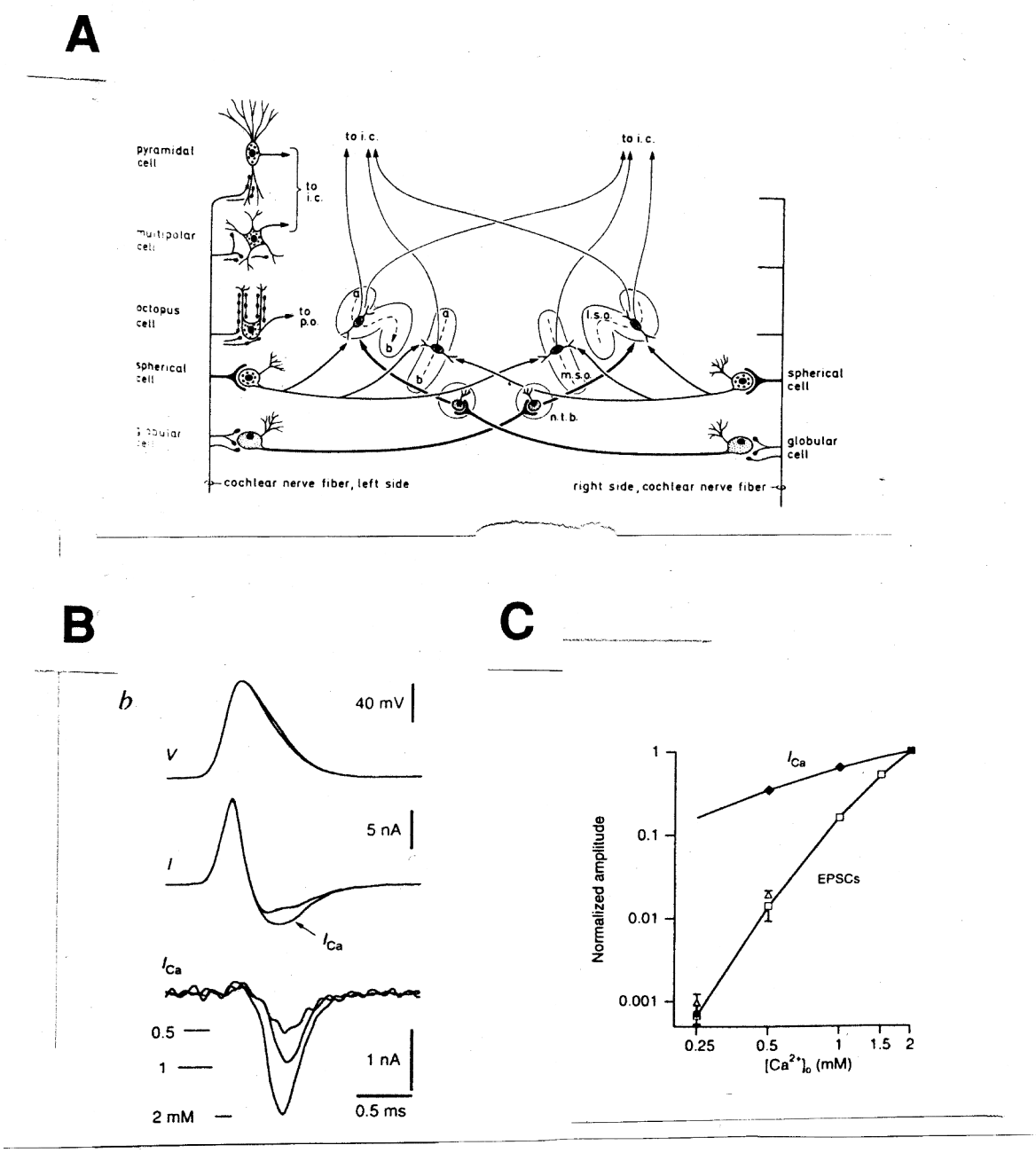

Figure 7-2. Calcium in afferents to the medial nucleus of the trapezoid body. A. Anatomical position of the nucleus of the trapezoid body (ntb) in the mammalian brainstem. Individual neurons in the NTB receive inputs from globular cells in the cochlear nuclei on both sides of the brain. Each axon form a calyceal ending on the NTB neuron. From (Brodal, 1981). B. Voltage (top trace), current (middle trace) and calcium (bottom traces) transients in presynaptic afferents. C. Amplitudes of the calcium transient and EPSCs as a function calcium concentration. The line through the points for the calcium transient were calculated by raising the amplitudes of the EPSCs to the one-fourth power, suggesting that transmitter release varies as the fourth power of intraterminal calcium concentration. From Borst and Sakmann (1996).

Intraterminal stores of calcium. In addition to a flux of calcium from the extracellular fluid into presynaptic terminals, axon terminals typically contain intracellular stores of calcium. Most cells contain sacs of membranes, the smooth endoplasmic reticulum. These membranes have both calcium channels and calcium pumps, so that they can sequester calcium. The signal that triggers release of calcium from the smooth endoplasmic reticulum is a rapid rise in intracellular calcium, rather than depolarization of the membrane. Thus, the rise in intracellular calcium that results from activation of voltage-gated calcium channels in the plasma membrane of the cell can result in a secondary rise in intracellular calcium. These changes can be demonstrated using calcium indicators. One preparation that is easily studied are sympathetic ganglia from frogs (Peng, 1996) which can be bathed in calcium indicators. The calcium channels found on the smooth endoplasmic reticulum are sensitive to the plant alkaloid, ryanodine, and are called *ryanodine receptors*. Thus, application of ryanodine to the frog sympathetic ganglion results in calcium transients (Fig. 7-3). Similarly, Purkinje cells from the cerebellar cortex show release of intracellular calcium that is mediated by ryanodine receptors (Kano et al., 1995), which can be demonstrated by applying the ryanodine receptor agonist, caffeine (Fig. 7-3B).

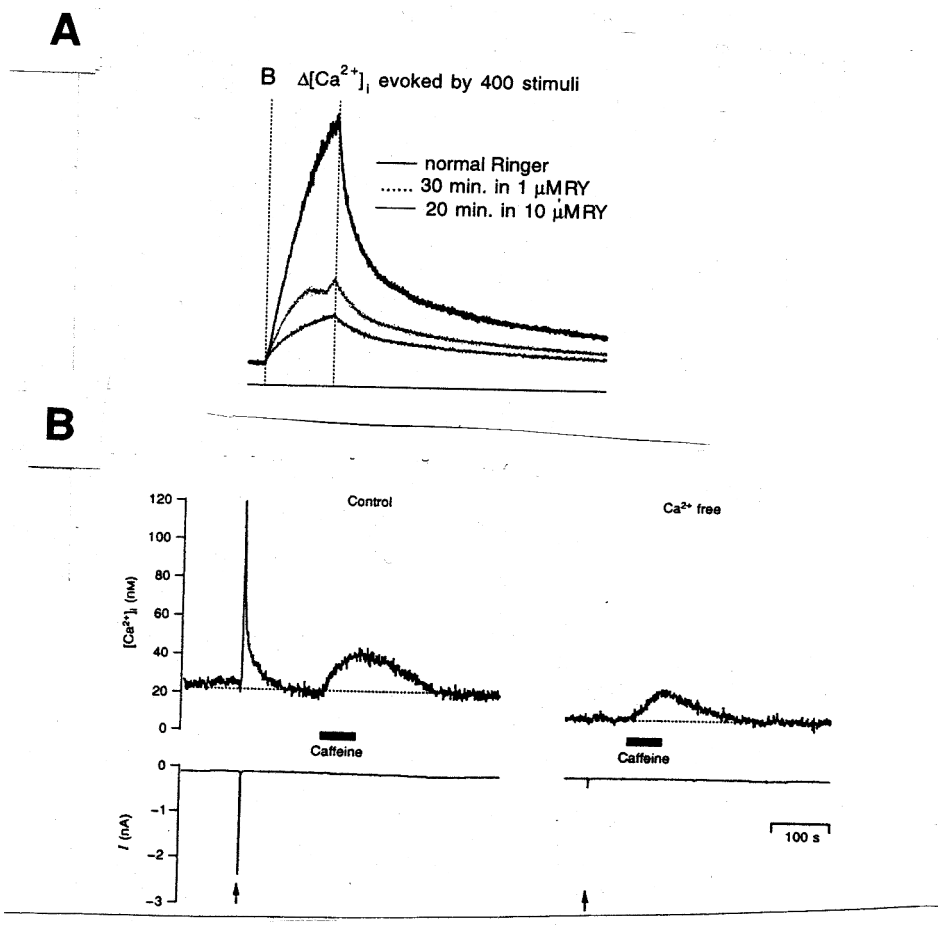

Figure 7-3. Release of calcium from intracellular stores. A. Release of intracellular calcium by ryanodine in frog sympathetic ganglion. Change in calcium concentration evoked in normal Ringer's solution and in two concentrations of ryanodine (RY). Including ryanodine in the bathing solution decreases the amplitude of the calcium change within terminals. From Peng (1996). B. Change in calcium concentration in following application of caffeine in control (left trace) and calcium free bath medium (right trace). Application of caffeine produces a slow calcium transient in both cases due to release from intracellular stores, but the fast calcium transient due to influx from the extracellular fluid is absent when the fluid does not contain calcium. From (Kano et al., 1995).

Removal of calcium. Calcium must, eventually, be cleared from the terminal and this process involves several different mechanisms. One is that calcium can be resequestered in the endoplasmic reticulum of the terminal. Another is that it can be pumped from the terminal by *calcium pumps* in the terminal membrane. The rate of calcium clearance is important because it plays

a role in shaping the information transmission properties of the axon. Two separate action potentials will result in the same number of vesicles being released from the presynaptic terminal only if the intraterminal calcium concentration triggered by the first action potential falls below some threshold level prior to the arrival of the second action potential.

Diffusion of calcium within the terminal. The local concentrations of calcium within the presynaptic terminal is determined by diffusion. Diffusion results from molecular interactions between molecules of some substance (such as calcium ions) in a fluid. This interaction is an example of *Brownian motion* in which individual molecules of solute collide with molecules of solvent. The thermal energy of the solvent molecules propels the solute molecules in some direction determined by the velocities of the molecules involved in the collision. Einstein (1956) showed that Brownian motion could be described mathematically as a *random walk* or *Markov process* in which each movement of the solute molecule is independent of its prior movement. The collisions result in solute molecules jumping forward in little jerks that last on the order of μsec. The observer does not have sufficient information about the states of the individual molecules to predict the motions of each transmitter molecule, but the average properties of the motion can be described. Berg (1983) provides an interesting and readable introduction to the mathematics of diffusion; Crank (1975) gives a more detailed treatment.

Treating diffusion as a Markov process leads to the diffusion equation

(7-1)
$$\frac{\partial C(x,t)}{\partial t} = D\frac{\partial^2 C(x,t)}{\partial x^2}$$

which describes the concentration, $C(x,t)$, of some solute as a function of distance, x, along the x-axis and time, t. Like the cable equation, it is a second order, partial differential equation. Derivation of the diffusion equation is similar to derivation of the cable equation in that it involves establishing a coordinate system and keeping track of the numbers of solute molecules at different points along the x-axis. It can easily be generalized to the diffusion of a substance in three dimensions. D is a constant, called the *diffusion constant*, which depends upon both the solute and solvent molecules. It has units of cm^2/sec or μm^2/msec. Calcium ions in water, for example, have a diffusion coefficient of 0.63 μm^2/msec (Blaustein and Hodgkin, 1969). Application of the diffusion equation to a particular problem requires specification of one or more boundary conditions. The equation can be solved analytically in some situations. It is identical to the equation that describes heat flow in structures with different geometries and Carslaw and Jaeger (1959) have tabulated solutions of the diffusion/heat equation for many common boundary value conditions.

The dynamics of calcium influx and extrusion can be quantified by modeling the presynaptic axon as a cylinder (Fig. 7-3). Zucker and Stockbridge (1983) used the diffusion equation in cylindrical coordinates

(7-2)
$$\frac{\partial Ca(r,t)}{\partial t} = \frac{D}{(\beta+1)r}\frac{\partial}{\partial r}\left[r\frac{\partial Ca(r,t)}{\partial r}\right]$$

to simulate the concentration of calcium within the axon as a function of space and time. Here $Ca(r,t)$ is the concentration of calcium in the terminal as a function of position, r, in the terminal and time, t. D is the diffusion coefficient of calcium in water and β is a parameter that represents the fraction of calcium

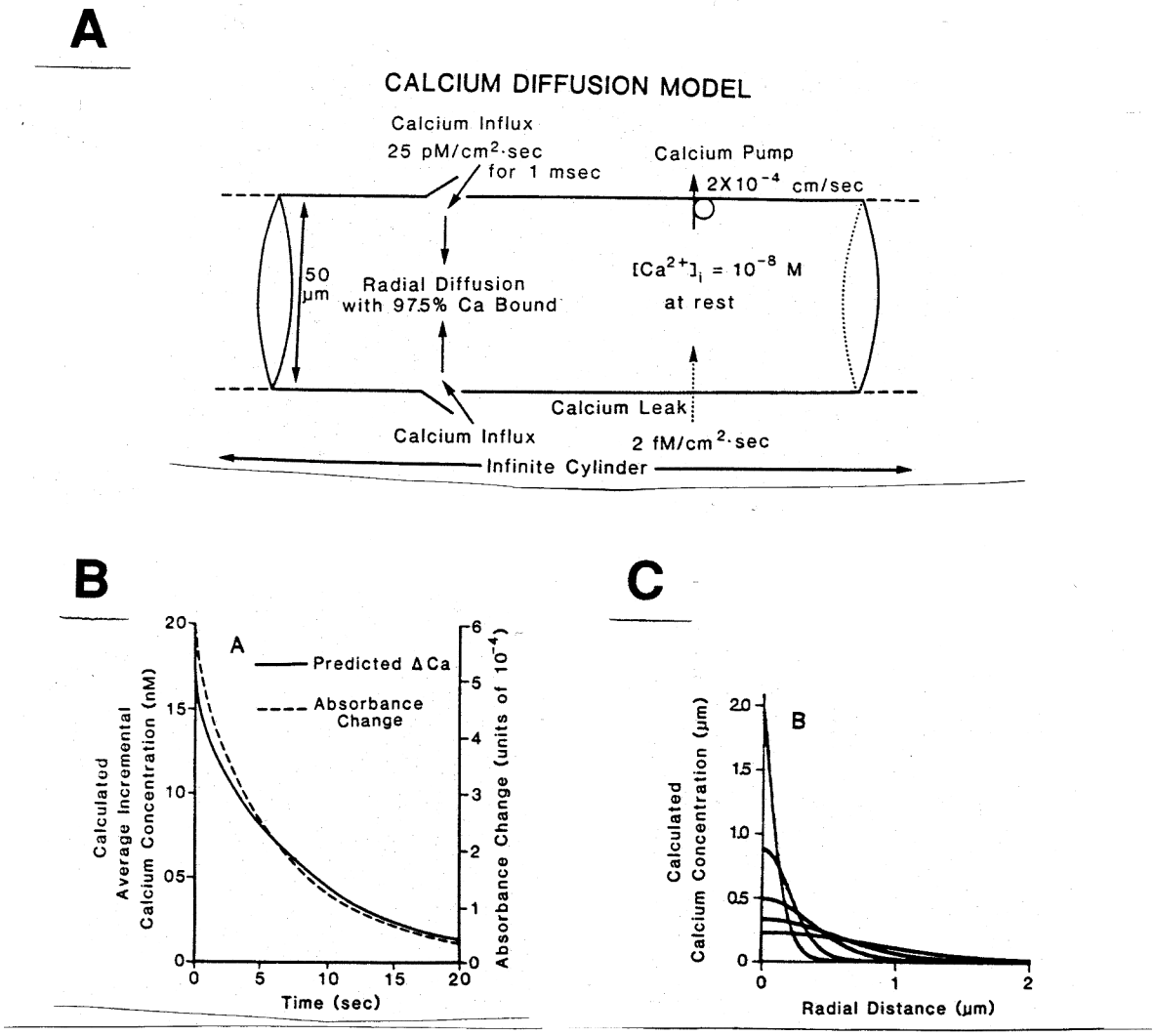

Figure 7-4. Ca^{2+} in squid stellate ganglion. A. Model of the presynaptic axon in squid giant synapse. B. Change in average calcium concentration as a function of time following activation of the axon. Axis on the left plots calculated change in calcium concentration. Axis on the right plots measured change in absorbance. C. Calculated concentration of calcium as a function of radial distance from the surface of the axon at several times. From (Zucker and Stockbridge, 1983).

bound to proteins, etc. within the terminal. Zucker and Stockbridge assummed that calcium influx occurs around the periphery of the axon through calcium channels and that extrusion of calcium occurs through calcium pumps in the plasma membrane. This diffusion problem is too difficult to solve analytically, so numerical methods were used to integrate the diffusion equation. The simulations predicted the time course by which the calcium concentration decayed following activation of the axon, as well as the spatial distribution of calcium within the axon.

Because axon terminals are so small, even the most sensitive imaging techniques are limited in their ability to visualize the diffusion of calcium within terminals. However, intraterminal calcium diffusion can be modeled using the diffusion equation. The simplest case is to represent the presynaptic membrane as a disk and position a voltage-gated calcium channel at the center of the disk. Distance from the center is represented by r. A brief influx of calcium is represented by a delta function. The solution to the diffusion equation for this condition is, thus, an impulse response function. Solution of the equation can, again, be approached using Laplace transform methods. The calculations are a bit more difficult, but show that the impulse response function is

(7-3) $$h(r,t) = \frac{C_o}{[4\pi Dt]^{3/2}} Exp\left\{-r^2 / 4Dt\right\} \quad .$$

Notice this is a Gaussian function of distance with $\sigma = \sqrt{4Dt}$, so the calculation leads to the intuitively reasonable conclusion that the concentration of calcium around the voltage-gated calcium channel will be a Gaussian function at each point in time. The Gaussian becomes broader as a function of time, and the calcium concentration will eventually be the same at each point along the axis.

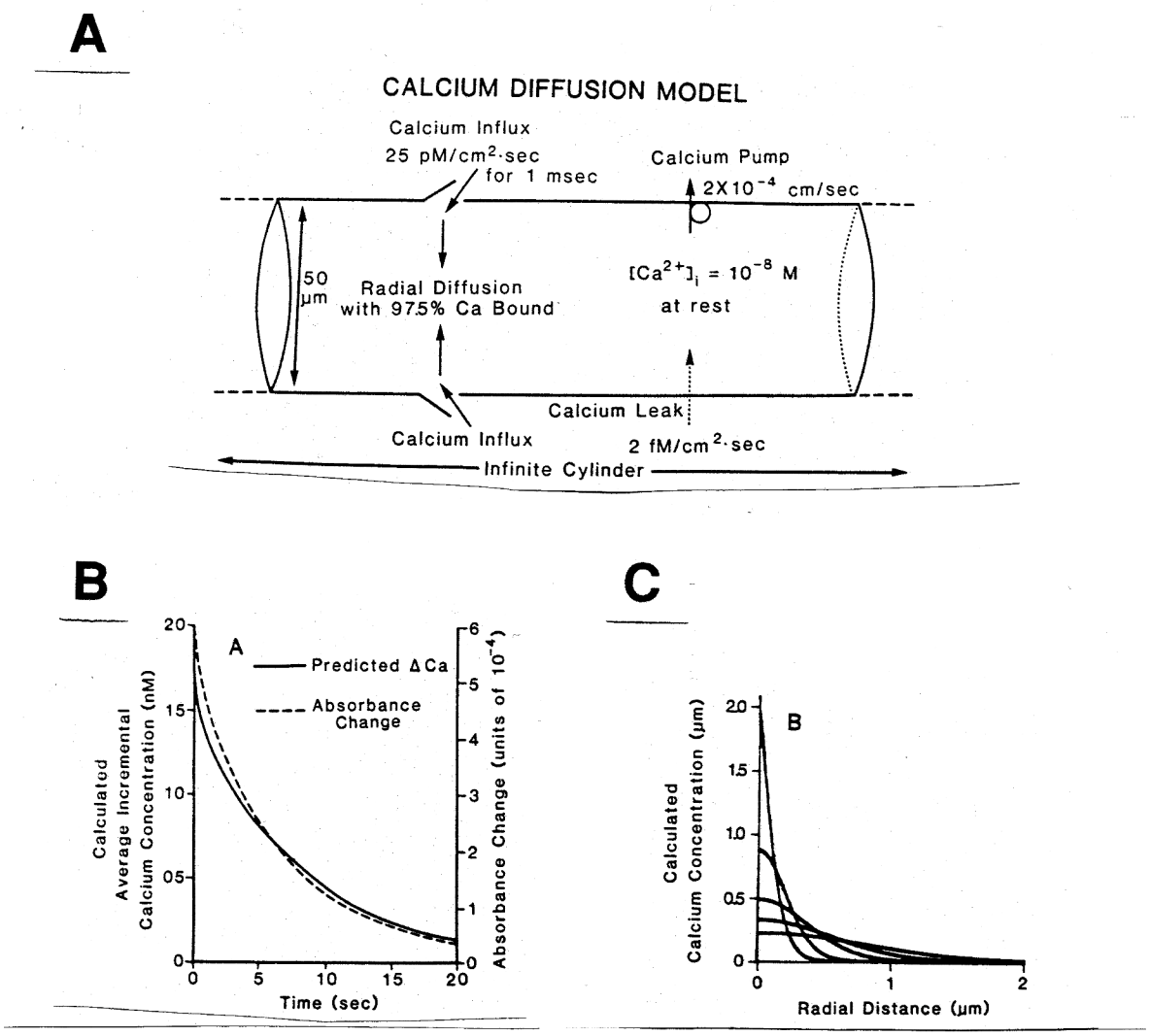

Figure 7-4. Intraterminal calcium domains. A. Presynaptic membrane showing a docked vesicle and several calcium channels admitting calcium ions in the sketch on the left. In the sketch on the right, a single channel is activated and produces a microdomain of calcium near the docked vesicle. B. Time course of the calcium transient relative to vesicle release (at zero time). C. Dimension of a calcium domain around the calcium channel and near the docked vesicle. From (Stanley, 1997).

The diffusion equation can be applied to a three dimensional coordinate system and solved in essentially the same way with comparable conclusions. The profile of calcium diffusion resulting from a more complex calcium transient can be predicted by convolving the impulse response function with the time-dependent

calcium profile. These calculations indicate that the opening of a single calcium channel results in a calcium microdomain relatively near a synaptic vesicle. The local calcium concentration increases rapidly to a peak near 100 μM in some cases. The calcium molecules begin to diffuse so that the local concentration begins to return to its resting level. Calcium is removed from the terminal through the combined action of calcium transporters and resequestration of calcium in the various intraterminal stores.

VESICLE RELEASE AND RECYCLING

The consequence of the rapid increase in calcium concetnration within the presynaptic terminal is the fusion of one or more synaptic vesicles with the presynaptic membrane. The dynamics of this process are difficult to study, but initial insights were obtained in elegant work by Heuser and Reese (1973). They bathed frog neuromuscular junction preparations in HRP. This tracer appears as an electron dense marker in electron microscopic preparations, so its location can be determined. Although the HRP was initially located solely outside of the terminal, it was found inside synaptic vesicles within the terminal after the preparation had been kept in the solution for several hours. They interpreted this to mean that HRP was being taken up from the extracellular fluid by a process of *endocytosis*. After the preparation had been maintained in the HRP solution long enough to load many of the vesicles with HRP, the extracellular fluid could be replaced with HRP-free solution and individual preparations sampled at time intervals. This process showed that HRP gradually was lost from vesicles and found again in the extracellular space. Vesicles are continuously recycled. As they move to the presynaptic membrane and fuse,

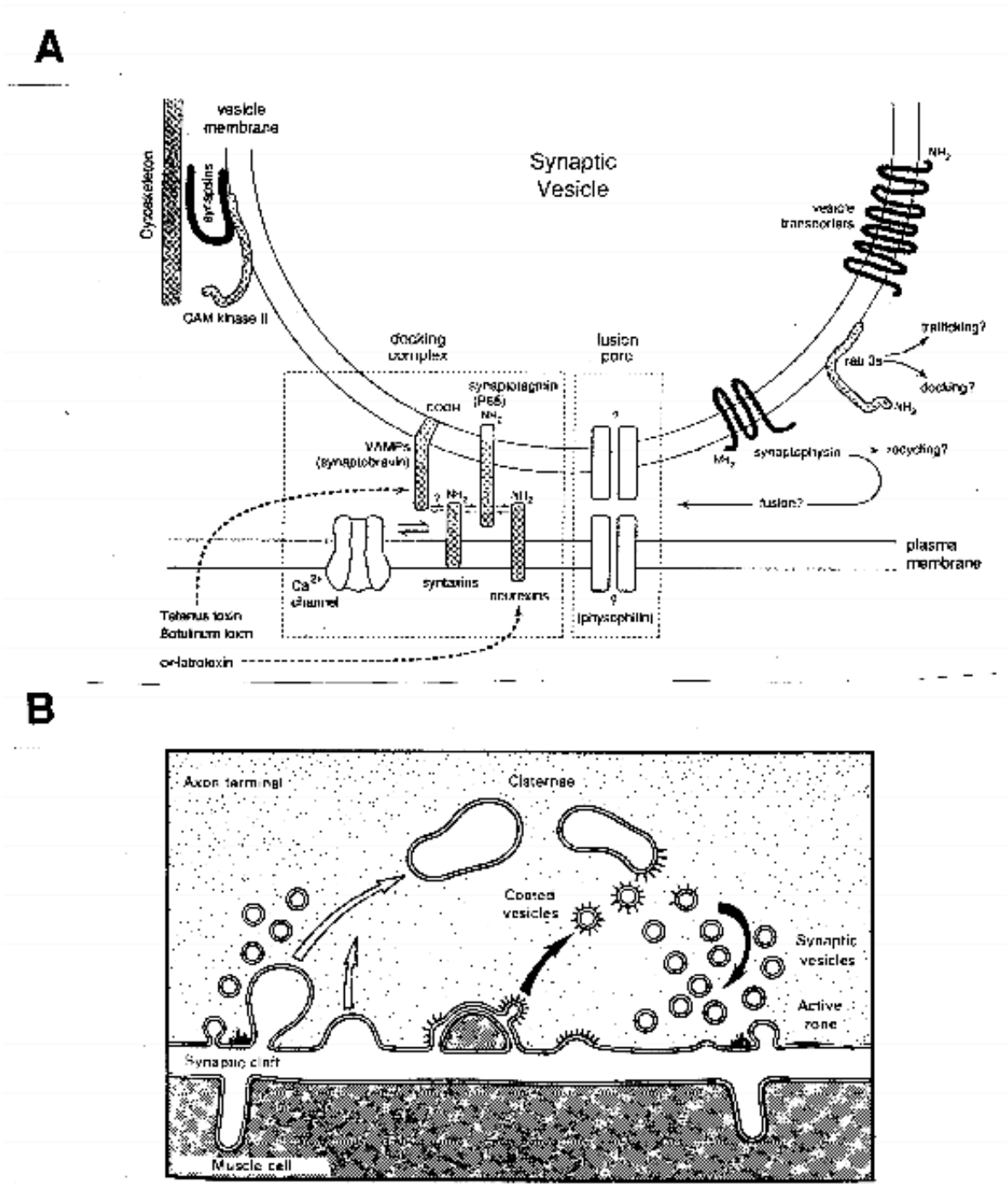

Figure 7-5. Release and recycling of synaptic vesicles. A. Proteins involved in vesicle docking and release are diagrammed. Part of a synaptic vesicle is shown in the upper part of the diagram. The plasma membrane of the presynaptic element of the synapse is shown at the bottom of the drawing. Various proteins are associated with the two membranes. From Jessel and Kandel (1993). B. The cycle of events by which synaptic vesicles fuse with the presynaptic membrane and are then retrieved from the membrane for recycling is illustrated for a neuromuscular junction. From Aidley (1987).

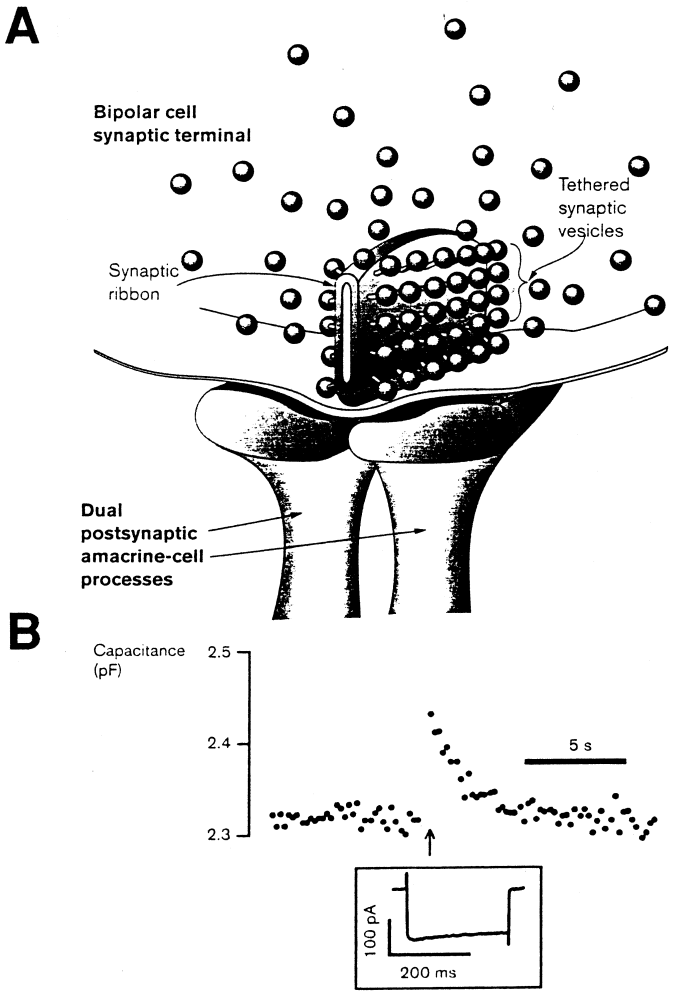

Figure 7-6. Capacitance measurements. A. Anatomy of a ribbon synapse in the synapse of a goldfish bipolar cell upon the dendritic process of an amacrine cell. The presynaptic density has the form of a vertical ribbon. Vesicles are tethered to both faces of the ribbon. B. Time course of the capacitance of the bipolar synapse when the synapse is activated. Arrow shows activation of synapse with a rapid increase in membrane capacitance due to fusion of vesicles. Capacitance decreases as vesicles are recycled. From Matthews (1996).

they release HRP into the synaptic cleft by *exocytosis*. HRP is susbsequently retrieved from the cleft by endocytosis.

The studies by Heuser and Reese characterized vesicle kinetics through a series of static snapshots. It is possible in some preparations to monitor the process of vesicle fusion and retrieval in real time by measuring the total capacitance of a cell (Neher, 1982; Lindau and Neher, 1988). This is done most readily in cells such as endocrine cells or *mast cells* (Henkel and Almers, 1996; Almers and Neher, 1987). These are relatively large cells found in the connective tissue of the body. They do not form synapses, but they resemble most other cells in containing vesicles that release their contents into the extracellular space by an exocytotic process. In particular, some of their vesicles contain *histamine*. This compound is a neurotransmitter in the central nervous system of vertebrates, but is released by mast cells as part of the allergic response to foreign compounds in the skin. The histamine-containing vesicles are small spheres of membrane which have a capacitance. Fusion of the vesicle increases the total capacitance of the mast cell. Assuming a specific membrane capacitance of 1 $\mu F/cm^2$, the amount of membrane added to the plasma membrane of the mast cell can be monitored by injecting small current steps into the cell and calculating the membrane time constant at frequent intervals. These capacitance measurements support the model in which vesicles add membrane to the plasma membrane of the cell during periods of exocytotic events and retrieve the membrane during periods of endocytotic events. Capacitance measurements have been applied to the synaptic terminals of bipolar cells from neurons (Matthews, 1996) such as goldfish retinas (von Gersdorff and Matthews, 1994). These terminals are relatively large, on the order of 10 μm in diameter, and contain approximately 60 ribbon synapses (Fig. 7-6). The large size of the terminals permits simultaneous capacitance measurements and monitoring of intraterminal calcium using Fura-2. A 250 msec depolarization produced a calcium current and a jump in capacitance of

about 154 fF (1 fF = 10^{-15} F), which corresponds to fusion of about 2,000 vesicles or about 30 vesicles at each of the 60 release sites.

The kinetics of vesicle release and recycling can also be characterized in neurons maintained in culture using the styryl dye FM1-43 (Betz and Bewick, 1992; Angelson and Betz, 1997). This dye can be added to the culture medium and is then taken up by the membrane of vesicles as they are recycled through endocytosis. Presynaptic elements are consequently stained by the dye, become fluorescent and appear as fluorescent *puncta* under the light microscope. Electron microscopy confirms that the dye is contained in the vesicles. As the presynaptic element is activated, vesicles are released and fluorescent puncta are destained. This method has been used to study transmission at individual boutons on hippocampal neurons in culture. Including FM1-43 in the bath produces puncta that contain fluorescent vesicles. Individual puncta can be activated by using a micropipette to apply a solution with high K^+ and Ca^{2+}, which depolarizes the terminal and facilitates vesicle release. EPSCs are recorded from the postsynaptic neuron using patch-clamp methods. Activation of the terminals produced EPSCs and presentation of trains of stimuli produced trains of EPSCs which declined exponentially in amplitude. The kinetics of recovery were studied by varying the rest interval between trains of repetitive stimuli.

A great deal has been learned about the details of vesicle recycling using methods from molecular biology (Söllner and Rothman, 1954; Robinson et al., 1994; Mundigli and Camilli, 1994; Südhoff, 1995). An impressive list of proteins have been implicated in the processes by which vesicles fuse with the membrane and are subsequently retrieved. Although there are details

characteristic of synaptic vesicle release and recycling, the basic process is similar to a number of other intracellular processes in which vesicles fuse and pinch off the Golgi apparatus or the processes of exocytosis and endocytosis in other cells. Analysis of the molecular mechanisms involved has been aided by studies on a number of preparations, including mutant forms of yeast that have perturbations of the mechanisms by which vesicles are transported through the Golgi apparatus. For our purposes, the important point is that vesicle release and retrieval is a kinetic process with a complexity comparable to, or exceeding, the complexity of receptor kinetics. Individual synapses must differ in the dynamics of the process in order to function properly. Synapses that customarily fire at high frequencies must be able to recycle vesicles very rapidly, while other synapses operate at a more leisurely pace. There must be subtle differences in the molecular properties of the proteins involved in vesicle release and retrieval between synapses, but these are not yet understood.

DIFFUSION OF NEUROTRANSMITTER IN THE SYNAPTIC CLEFT

The consequence of a vesicle fusing with the presynaptic membrane is that thousands of transmitter molecules appear in a restricted volume in the synaptic cleft. Proper function of the synapse imposes several competing design features (Eccles and Jaeger, 1957). The transmitter molecules must diffuse through the cleft and reach the receptors on the postsynaptic membrane with reasonable speeds. The time required for transmitter to reach the receptors limits the speed of information transfer. If it takes hundreds of msec for transmitter to reach the receptors, the rate at which the synapse could transmit information would be severely limited. This requirement favors synapses with narrow synaptic clefts, so the diffusion time is small. Once

transmitter molecules bind to the receptors, they open channels that allow ion fluxes resulting in postsynaptic currents. This means there must be sufficient space in the cleft to permit current flow. One way to decrease diffusion time would be to place the presynaptic membrane very close to the postsynaptic membrane. However, this would eventually increase the resistance of the cleft and impede current flow. Finally, some mechanism to remove transmitter from the cleft is required. Otherwise, receptors might be continuously activated by transmitter released by one action potential and the postsynaptic element would be unable to response to subsequent action potentials in the presynaptic element. Transmitter can be cleared from the cleft by three basic mechanisms. The first is that it can diffuse from the cleft into the extracellular space that surrounds the synapse. The second is that some synapses contain enzymes that degrade the transmitter in the synaptic cleft. We have already seen an example of this in the neuromuscular junction in which molecules of the enzyme acetylcholinesterase are bound to the basal lamina that occupies the middle of the cleft. Finally, many synapses have integral membrane proteins called *transporters* that take up transmitter molecules from the cleft and transport them into the presynaptic element, where they can be repackaged in recycled vesicles.

The movement of transmitter molecules within the cleft is described by the diffusion equation. To get a general idea of this process, let's consider the simple, and somewhat idealistic, problem of describing the flow of transmitter from the cleft into the extracellular space (Fig. 7-7). We place the edge of the cleft at $x = 0$ on the x-axis (Fig. 7-7A). Extracellular space thus extends to the right along the x-axis. We assume that the transmitter concentration is zero at the edge of the cleft prior to vesicle release and instantaneously increases to a

constant value, C_o, at the edge when the vesicle is released. The concentration of transmitter at the edge of the cleft is, thus, given by the step function

(7-4) $$C(0,t) = 0, t \le 0 \quad \text{and} \quad C(0,t) = C_o, t > 0 \quad .$$

Our intuition is that transmitter concentration will gradually increase along the x-axis with time. We use the strategy developed earlier in the chapter and rely upon Laplace transform methods. We take the Laplace transform of each term in Equation (7-1), remembering to treat the spatial coordinate, x, as a constant since we are moving from the time domain to the Laplace transform domain.

(7-5) $$\mathrm{L}\left\{\frac{\partial C(x,t)}{\partial t}\right\} = \mathrm{L}\left\{D\frac{\partial^2 C(x,t)}{\partial x^2}\right\}$$

and

(7-6) $$sc(x,s) - C(0,0) = D\frac{d^2 c(xs)}{dx^2} \quad , \quad c(x,s) = \mathrm{L}\{C(x,t)\}$$

so we now have the ordinary differential equation

(7-7) $$\frac{d^2 c(x,s)}{dx^2} - \frac{s}{D}c(x,s) = 0 \quad .$$

Again by analogy with the cable equation, the solution to this equation is

(7-8) $$c(x,s) = ae^{+x\sqrt{s/D}} + be^{-x\sqrt{s/D}}$$

where a and b are constants. Since the transmitter concentration should not approach infinity along the x–axis, $a = 0$ and

(7–9) $$c(x,s) = be^{-x\sqrt{s/D}}$$

To evaluate b, we use the fact that the Laplace transform of the step function is $1/s$ so

(7–10) $$c(0,s) = \mathrm{L}\{C(0,t)\} = C_o / s \quad , \quad t > 0 \quad .$$

From Equation (3–73), we also know that $c(0,s) = be^{\circ}$. Thus, $b = C_o / s$ and

(7–11) $$c(x,s) = \frac{C_o}{s} Exp\{-\frac{x}{\sqrt{D}}\sqrt{s}\} \quad .$$

We are almost done, except we have to move from the Laplace transform –domain back into the time–domain, which we do by using a table of Laplace transforms to find the inverse Laplace transform of Equation (7–11)

(7–12) $$C(x,t) = \mathrm{L}^{-1}\left\{\frac{C_o e^{-x\sqrt{s/D}}}{s}\right\} = C_o\left\{1 - \frac{2}{\sqrt{\pi}}\int_0^{x/\sqrt{4Dt}} e^{-u^2}\,du\right\} \quad .$$

Notice that the integral in Equation (7–12) is actually the error function. We can, consequently, express the solution to the problem in terms of the error function and look up values for the error function in standard tables. However, we can figure out the general form of the solution by inspecting Equation (7–12). As $t \to 0$, the error function term approaches 1 for all points along the x–axis. As $t \to \infty$, the error function term approaches 0 for all points along the x–

axis. For intermediate time values, the concentration of transmitter declines along the x-axis.

The relevance of this calculation to real synapses is rather limited by the geometry of the synaptic cleft. We have already seen, for example, that the postynaptic membrane undulates to form a series of postjunctional folds in the neuromuscular junction. The number, size and distribution of these vary between species and, in some cases, the spacing between junctional folds varies along the length of the junction. Many postsynaptic elements protrude into the presynaptic element, so the cleft has a very intricate geometric strucuture. It is also quite common for synapses to be encased in glial sheaths, so the geometry of the path by which the transmitter diffuses from the cleft is also complicated. Analytic solutions to the diffusion equation are, thus, impossible in most realistic cases. However, an alternative approach is to use *Monte Carlo methods* (Rubenstein, 1981) that follow the movements of individual molecules. Rather than trying to solve the diffusion equation for a population of N molecules, the diffusion equation is used to predict the average trajectory of an individual molecule for a short period of time. Large numbers of simulations (typically thousands or tens of thousands) are run using random assignments of initial conditions to build up a picture of how a population of molecules would be distributed in space and time. Monte Carlo methods can be efficiently applied to synapses with any geometry, and also with receptors distributed in any desired pattern in the postsynaptic membrane. The disadvantage of the method is that the computational demands are significant and may require the use of a supercomputer.

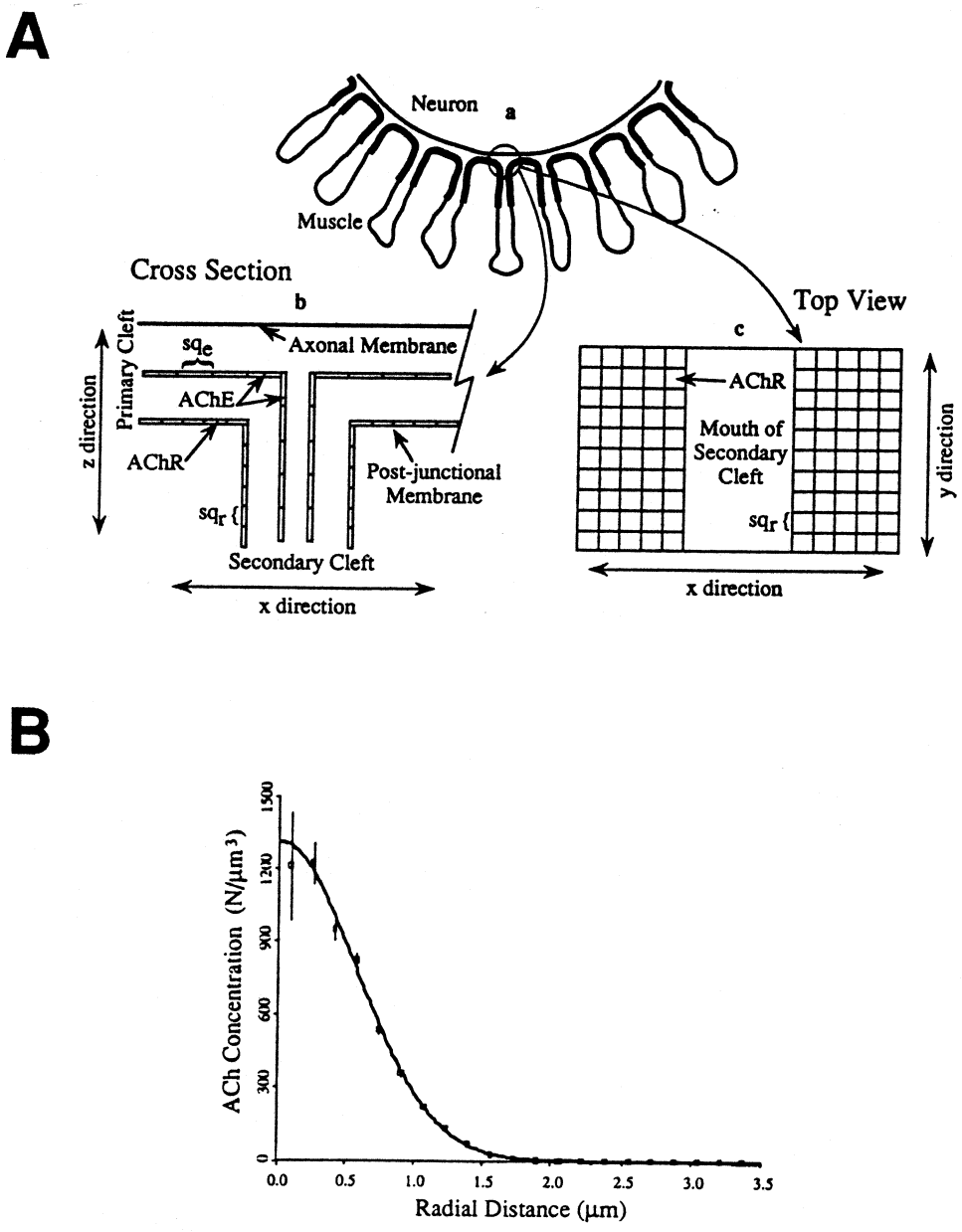

Figure 7-8. A. Model of a neuromuscular junction. The top sketch shows the junction in cross section. Dark lines represent concentration of acetylcholine receptors on the crest of the post-junctional folds. The lower sketches show representations of the geometry of the junction in cross section and in top down views. B. Calculated concentration of acetylcholine as a function of radial distance in the cleft measured from the release site. From Bartol et al. (1991).

Both numerical methods and Monte Carlo simulations have been used to study the dynamics of transmitter in the cleft for a number of synapses, with the neuromuscular junction and glutaminergic synapses attracting particular attention. Wathey et al. (1979), for example, used numerical methods to model the neuromuscular junction (Fig. 7-8). The cleft was represented as a disc that was open to the extracellular space at its edges. It was assumed that a vesicle instantaneously releases acetylcholine into the cleft and the diffusion equation was used to describe the concentration of acetylcholine in the cleft as a function of position and time. Degradation of acetycholine by acetylcholinesterase was represented by the kinetic equations for enzyme-subtrate reactions. (These are the *Michaelis-Menton equations* that are discussed in all biochemistry textbooks.) Transmitter interactions with nicotinic receptors were described by a kinetic scheme of the kind discussed above. The model was used to calculate the fraction of receptor molecules binding one or two molecules of acetylcholine as a function of time and to examine the relative contributions of diffusion from the cleft and degradation to transmitter clearance. The simulations suggest that nearly 60 % of the receptors are doubly bound by acetylcholine within a fraction of a millisecond, and that enzymatic degradation will be responsible for clearing approximately three times as much transmitter from the cleft as diffusion. Bartol et al. (1991) used Monte Carlo methods to model neuromuscular junctions and were able alter the size and spacing of junctional folds in their model. The simulations suggest that the presence of folds decreases the efficiency of acetylcholine binding, so some alteration of kinetic parameters would be required to maintain the maximum amplitudes of EPPs. To appreciate the potential functional significance of this finding, look back at Figure 5-1. Notice that eventhough each of the synapses illustrated is serving the same basic function of transmitting information from a

motoneuron axon to a muscle fiber, the remarkable variation in geometry between the terminals suggests that there are likely major variations in kinetics of transmitter diffusion.

Monte Carlo methods have also been used to simulate the time course of glutamate in the cleft of synapses that use the excitatory amino acid, glutamate, as a neurotransmitter (Bartol et al., 1991; Clements, 1996). The simulations suggest that glutamate remains in the cleft for a relatively short period of time, probably less than 1 msec. The average transmitter concentration in the cleft falls to about 50 % by 50 μsec and to 10 % by 500 μsec. The diffusion coefficient of the transmitter seems to be more important in determining the rate of clearance than does cleft geometry. The clearance rate initially follows an exponential time course determined by diffusion from the cleft, but later follows an exponential time course with a longer time constant that is determined by the binding of transmitter to receptors. Glutamate clearance has been examined experimentally using EPSCs evoked in rat hippocampal neurons. The procedure was to use a competitive antagonist of the glutamate receptor (d-aminoadipate or D-AA) which unbinds rapidly from the receptor. Saturating the preparation with D-AA completely blocks EPSCs because glutamate molecules are unable to compete with the antagonist in accessing receptors. The concentration of D-AA was systematicaly reduced and the increased ability of glutamate to access receptors measured. A kinetic model that involved binding of both D-AA and glutamate to the receptors could be used to estimate the time course of glutamate in the cleft. The time course followed a double exponential curve in which the amplitudes of the two components were 2.7 mM and 0.4 mM and the time constants were 100 μs and

2.1 ms. Both the theoretical and experimental results suggest that glutamate is cleared quickly from the cleft.

An issue that has attracted particular attention is whether or not a single vesicle releases enough transmitter molecules to completely saturate all of the postsynaptic receptors (Frerking and Wilson, 1996; Clements, 1996). If it does, the flexibility of the synapse would be decreased since release of additional vesicles within a small time window would have no additional effect on the postsynaptic element and the quantal peaks expected in a statistical analysis would not be seen. You will recall from Chapter 5 that demonstrating quantal peaks has been problematic for many central synapses, so this is a real issue. Holmes (1995) approached this problem by constructing a model of a synapse that uses glutamate. Thickness was ignored in modeling the cleft and a one-dimensional diffusion model was used. Glutamate does not undergo enzymatic degradation in the cleft, but there are specific transporters for glutamate both on the presynaptic membrane and on the membrane of glial cells that surround the synapses. Glutamate uptake by the transporters was modeled using Michaelis-Menton kinetics. The simulations suggested that a single vesicle can release enough transmitter to bind to or saturate between 60 % - 90 %, or more, of the receptors. The simulations were sensitive to many of the parameters used, so the degree of saturation occuring in real synapses can be expected to vary.